(Preprint) AAS 11-146

TRAJECTORY DESIGN CONSIDERATIONS FOR SMALL-BODY TOUCH-AND-GO

Mark S. Wallace, Stephen Broschart, Eugene Bonfiglio, Shyam Bhaskharan, Alberto Cangahuala*

"Touch-and-Go," or TAG, is an approach to small-body surface interrogation missions in which the spacecraft descends to the surface, remains in contact for a short time, and then ascends without coming to rest. Appropriate trajectory design solutions to support TAG missions vary widely based on the spacecraft dynamics, small-body environment, spacecraft and ground systems capabilities, and mission objectives. This paper discusses various factors that are considered during the process of developing a TAG mission trajectory and presents a few case study examples to demonstrate how TAG trajectories may vary from mission to mission.

INTRODUCTION

In the context of a mission to an asteroid, comet, or small planetary moon, "Touch and Go," or TAG, refers to a surface mission approach in which the spacecraft descends to make brief contact (on the order of seconds) with the surface before ascending to a safe location. Missions that require contact with the surface, such as sample return missions or demonstrations of surface interaction hardware, may consider TAG as an alternative to a more traditional "landing" to avoid the need for landing hardware and mitigate concerns about rough surface topography. TAG is currently of particular relevance with respect to the small-body mission objectives of both the robotic[1,2] and human exploration[3,4] communities within NASA.

Successful TAG strategies require a carefully designed system architecture involving many subsystems and design disciplines, including trajectory design, guidance algorithms, attitude control systems, navigation, sensors, surface interaction hardware, and fault protection. In order to keep a manageable scope, this paper will focus on the considerations that must be made in only the trajectory design area. TAG trajectory design (as well as the rest of the architecture) is ultimately driven by the mission science objectives, the capabilities of the spacecraft and mission ground systems, and the characteristics of the small-body environment. Because of the endless variety that exists in these mission characteristics, TAG trajectory solutions end up looking very different from mission concept to mission concept. This paper discusses the trajectory design choices and their drivers that are considered during the development of a TAG mission.

* Autonomous Systems Division, Jet Propulsion Laboratory/California Institute of Technology, 4800 Oak Grove Drive, Pasadena, CA 91109.

The paper begins with a definition and discussion of TAG from the perspective of a trajectory designer. The following sections present a number of considerations for TAG trajectory design grouped into the areas of spacecraft dynamics, the small-body environment, spacecraft and ground system capabilities, and mission objectives. A discussion follows that maps the TAG trajectory design choices to the various considerations detailed above. Finally, historical examples and example design exercises for a few case studies are presented: the Near-Earth Asteroid Rendezvous (NEAR) mission descent to Eros, the Hayabusa TAG at Itokawa, TAG at the Martian moon Deimos, TAG at Comet Tempel 1, and TAG at the binary asteroid 1996 FG3.

TAG TRAJECTORY DESCRIPTION

In the context of a small-body mission, a "touch-and-go" trajectory sequence, or TAG, refers to a spacecraft trajectory that includes a brief physical contact between the spacecraft and the small-body surface. TAG differs from a descent or landing trajectory in that the contact only lasts a matter of seconds and the spacecraft never comes to rest on the surface. The objectives of a TAG design are driven by the science and engineering objectives of the mission. Generally speaking, the primary requirement on trajectory design can loosely be stated as: "safely and reliably deliver the spacecraft to a specified contact state without jeopardizing the expected science and/or engineering return".

The TAG architecture is often associated with sample return mission concepts. Significant quantities of surface regolith can be obtained during a brief surface contact event using boom or robotic arm mounted devices. Depending on the science objectives, the TAG approach can offer benefits over landing at a small body; for example, no landing/contact hardware, less sensitivity to unknown surface properties, and less-restrictive power and communications requirements. The same benefits also apply to other missions that require a very-close (on the order of meters) approach to a surface target (e.g., projectile dropping or high-resolution imaging).

For the purpose of the discussion in this paper, the TAG trajectory is broken into four stages: staging, descent, contact, and ascent. Staging refers to the portion of the trajectory before the commitment is made to go to the surface. Examples of staging strategies are a slow flyby, a safe orbit, or an active station-keeping trajectory. Descent is the portion of the trajectory after a commitment to the surface has been made until contact. Contact refers to the portion of the trajectory when the spacecraft is touching the surface and thus influenced by additional forces and moments introduced by this contact. Ascent is the portion of the trajectory when the spacecraft moves from contact to some safe trajectory away from the surface. Figure 1 illustrates these four stages. Discussion of the design choices associated with each phase follows in a later section.

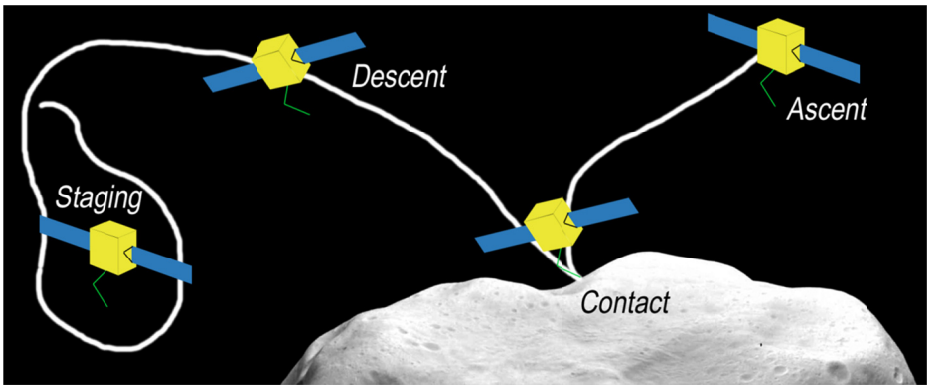

Figure 1: Touch-and-Go includes four phases: staging, descent, contact, and ascent

DESIGN DRIVERS: DYNAMICS

The dynamics of a spacecraft in the vicinity of a small body are quite complex due to accelerations arising from a non-spherical gravitational potential, differential gravity (a.k.a., tidal forces) of distant sources (e.g., the Sun), solar radiation pressure (SRP), and, in some cases, comet outgassing. The relative importance of these forces will vary significantly depending on the properties of the targeted small body, the operating range with respect to the body, and the spacecraft design. Discussion of these dynamics is given in References 5, 6, 7, 8, and 9. Figure 2 notionally illustrates the balance between the above forces (less outgassing) as a function spacecraft of position relative to the small body. The TAG trajectory phases closest to the surface will be dominated by the gravity of the small body, but the other phases will likely transition to and from this region from other areas of dominance.

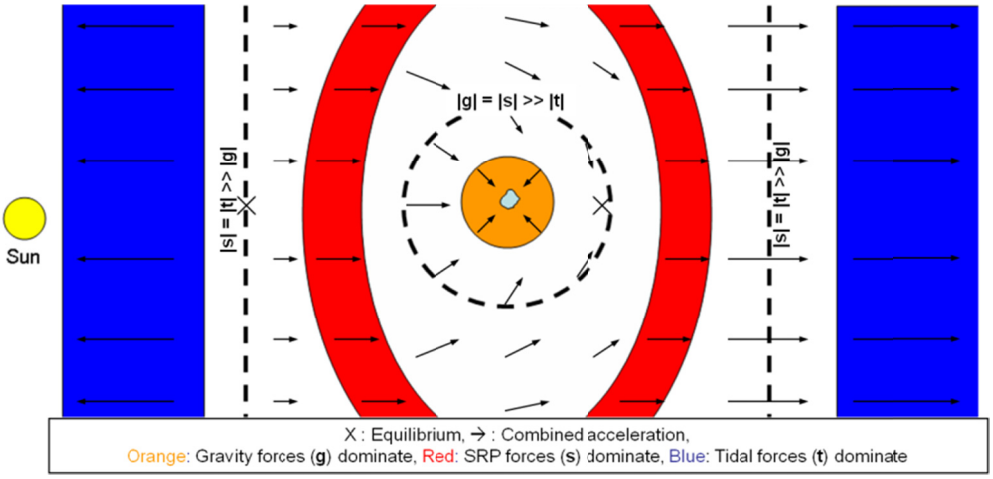

Figure 2: The forces that dominate the motion near a small body vary with position (not to scale).

Gravity. Small bodies are non-spherical in shape. Thus, a pointmass potential model is appropriate only when relatively far from the body (i.e., not for TAG) or for preliminary analysis purposes. A detailed TAG design generally requires consideration of a higher order gravity model in order to model dynamics down to the surface. Spherical harmonics[10] can model the gravity of a body outside of the oblateness, or maximum radius, of the body, but other gravity models must be used to simulate the gravity within this radius. Methods for modeling gravity within the Brillouin sphere include surface integrals[11], polyhedral gravity models[12], and potentials using the moments and products of inertia[13].

Solar Radiation Pressure. Because the gravity of small bodies is often very small, SRP is, in many cases, the dominant spacecraft acceleration when in proximity (but not too close) to a small body (see Figure 2). This force on the spacecraft depends on the spacecraft surface reflectance properties, as well as the range and attitude with respect to the Sun. A simplified model where SRP is modeled as acceleration in the anti-Sun direction is often used[6].

The most notable effect of SRP is that it destabilizes most orbits when the acceleration is significant with respect to gravity via an increase in orbit eccentricity[8,14]. For bodies on the smaller end of the scale (roughly less than 2 km diameter), terminator orbits[15] and a few other isolated orbit solutions[16] are the only known spacecraft orbits that are stable over long durations.

Differential Gravity or Tidal Forces. These forces arise from distant, third-body gravitational accelerations, e.g., gravity of the Sun or a planet. For solitary comet and asteroid missions, these

forces have little relevance to TAG as they are only important far from the surface. For planetary moon missions however, these forces may have significant effect on the orbital dynamics.[17]

Coriolis and Centrifugal Forces. In the descent and contact stages of TAG, spacecraft dynamics are generally considered in a coordinate frame that rotates with the surface. Coriolis and centrifugal accelerations are introduced in these dynamics. The Coriolis acceleration acts to turn the spacecraft away from its heading and increases linearly with the rotation rate of the body and the speed of the spacecraft. Fast rotating bodies may require different trajectories and maneuver frequencies than slow rotators to counter the Coriolis effect.

The centrifugal force accelerates the spacecraft orthogonal to the small-body spin vector. For a rapidly rotating body, this effect may overwhelm gravity all the way down to the surface, necessitating an atypical approach to TAG. By considering these forces, equilibrium points (in the rotating frame) and synchronous orbits can be identified that may have application to TAG staging.

Outgassing Acceleration. At a comet, the dust and gas rising off the surface will impinge upon the spacecraft, creating acceleration away from the comet. Comet outgassing quantities are known to be variable with range from the Sun and from orbit to orbit. The distribution of outgassing intensity over the comet surface is known to be non-uniform. This acceleration is very difficult to predict, but a TAG trajectory at a comet must be robust to the expected possibilities.[9]

Secondary Bodies. Small bodies often exist as binary (or trinary) pairs. In this case, the irregular gravitational potential of both bodies must be considered. In this case, the dynamics can generally be thought of in terms of the restricted three-body problem,[18] though when modeled to high fidelity, the coupled motion of the two bodies is complex.[19]

Dynamical Uncertainty. Large uncertainties in the dynamical parameters, particularly those related to gravity and comet outgassing, are a characteristic of the vast majority of small-body missions, especially during the development stages. Typical Earth-based optical observations can only roughly determine a small-body shape (radius to approximately a factor of 2.6x for unknown albedo between 0.06 and 0.4)[20] and give no information about density, which leaves significant uncertainty in mass and higher-order gravity harmonics. For objects that come near the Earth, shape can be determined accurately using radar sounding techniques,[21] but density is still unknown (except for multi-body systems). For very large small bodies (e.g., Ceres and Vesta), mass can be estimated by observing close approaches with other asteroids. The rotation pole, which is important for computation of Coriolis and centrifugal forces, takes repeated measurements over a long baseline to determine from Earth. The variation in the pressure of outgassing products emitted from the surface of a comet varies both across time and surface location and is virtually unknowable during mission development. Upon arrival at the small body, the process of navigation and estimation reduces the uncertainty in the dynamical parameters, though significant residual uncertainty may still exist due to the limitations of the available measurements.

Since significant uncertainty is an unavoidable part of small-body mission operations, TAG trajectory designs must be robust to the range of possibilities in all uncertain parameters. Based on the available scientific observations, the expected range of parameters should be characterized. The TAG trajectory strategy should then be validated across the range of possibilities and the spacecraft fuel budget and timeline should be sized accordingly. Figure 3 shows example histograms describing the uncertainty in various dynamical characteristics at comet 9P/Tempel 1 which could be used as the basis of a Monte Carlo study of TAG trajectory performance.

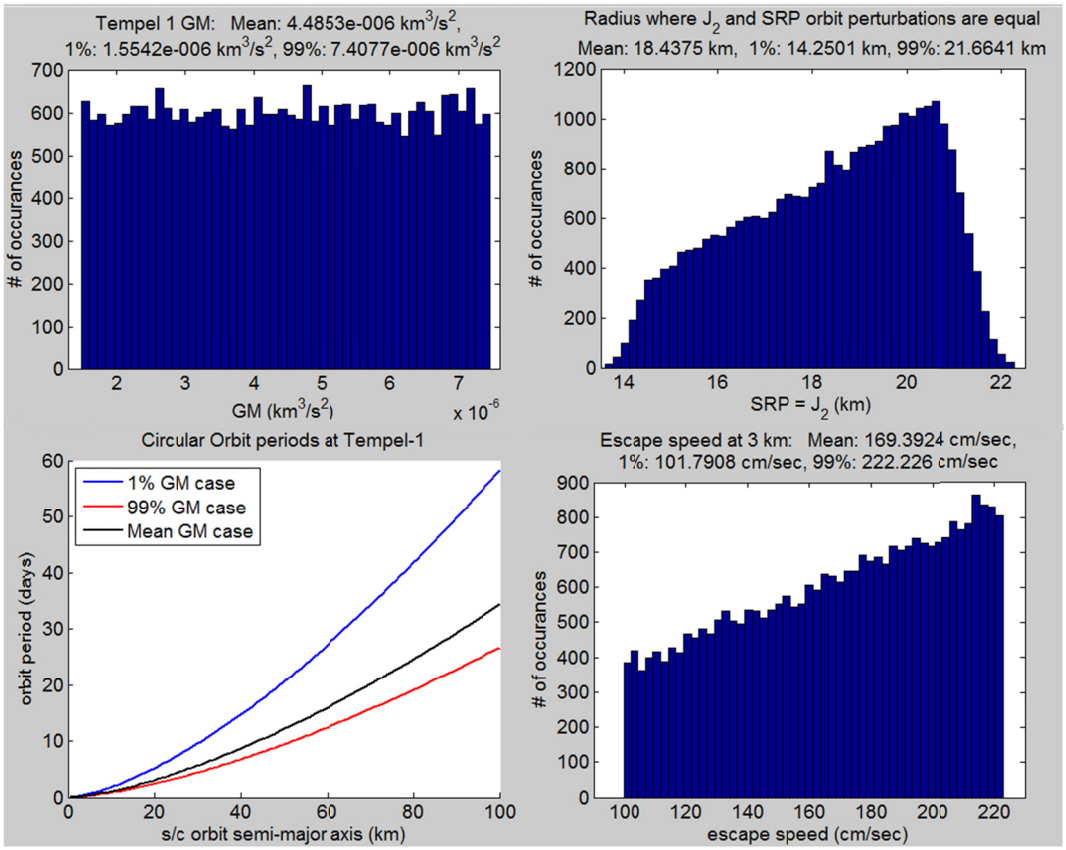

Figure 3: Histograms representing uncertainty in the dynamical environment near comet 9P/Tempel 1: (top left) GM, (top right) orbit size where J2 and SRP perturbations are equal,[14] (bottom left) circular orbit period, and (bottom right) approximate surface escape speed.

DESIGN DRIVERS: ENVIRONMENT

In addition to the dynamics, the environment in which TAG is to occur must also be considered in the trajectory design. The small body environment encompasses both the proximity hazards and the characteristics of the small body surface itself.

Orbiting Debris and Dust. Dust and debris in orbit around the small-body or that rises off the surface due to TAG is a potential hazard to spacecraft functionality that should be assessed by a space mission before approaching to close proximity. In most cases, orbiting debris is not a concern. Hamilton and Burns[22,23] have demonstrated that SRP and tidal forces will strip away orbiting debris far from the body relatively quickly. The unstable orbital environment introduced by the irregular gravity field and SRP tends to quickly eliminate small debris close to the body.[8, 14, 24] The exceptional cases involve large orbiting "secondaries" that are not strongly destabilized by SRP. Debris lifted from the surface by a recent impact may persist for timescales on the order of days to weeks,[25, 26] though most will be immediately ejected due to low surface escape velocities.

Dust lifted by spacecraft activity during the TAG event is a concern because of the close proximity of the spacecraft to the source. The effect of this dust on important spacecraft functionality such as power generation, navigation, and actuators should be assessed during development. The impact of dust lifted from the surface by comet outgassing activity should be similarly considered. Outgassing may also lift larger rocks from the surface (tens of centimeters and larger) at low speeds that could damage the spacecraft if impact occurs.

Landing Site Availability and Topography. For TAG, a smooth and obstacle-free surface location of appropriate size is desired to accommodate uncertainty in the contact delivery state. For almost any particular mission target, the size and distribution of surface hazards such as boulders and cliffs is completely unknown/unknowable during the mission planning phase, though it can be reasonable expected that many such hazards exist. In order to maximize the likelihood of finding a suitable TAG location on an unknown body, the position delivery errors to the landing site should be minimized and the trajectory design should allow for landing sites that span as much of the body as possible.

The sub-meter level surface topography at the touchdown location has significant influence on the dynamics of the spacecraft during contact,[27] which in turn affects the dispersion in ascent trajectories. These small scale variations in slope may remain unknown even after TAG.

DESIGN DRIVERS: SPACECRAFT AND GROUND SYSTEM CAPABILITIES

Beyond the natural dynamics and environment, the capabilities of the spacecraft and the supporting ground infrastructure and personnel also drive the TAG trajectory design.

Navigation and maneuver capabilities. Trajectory design must respect limitations on knowledge of the spacecraft state and the turnover time needed to implement correction maneuvers. These quantities are derived from the navigation/operations strategy, maneuver execution errors, and dynamics modeling uncertainties. If navigation and maneuver design during TAG are to be done by ground personnel, then time must be allowed between maneuvers for that processing to occur (including round-trip light-times). An autonomous navigation and maneuver design system allows for more correction maneuvers during TAG (due to a faster design turnover time) and, thus, a smaller dispersion in surface contact state than a ground-based approach.[28] Navigation and maneuver execution considerations also drive the number of burns planned, burn altitudes, and may require portions of the trajectory to be biased to avoid undesirable outcomes.

Some form of optical navigation is typically used for close-proximity operations at a small body.[29,30] The need for appropriate lighting for this data type may introduce geometric constraints on the trajectory that require that the spacecraft reach the contact site at some specific solar phase angle, or approach it from some particular direction.

Power and Communications. The end-to-end trajectory is subject to larger geometrical constraints with respect to power and communications. Spacecraft batteries have a limited capability, and either the TAG trajectory timeline must fit within the battery depth-of-discharge constraints or the spacecraft must be kept power-positive. In addition, it may be desirable to maintain continuous communication with Earth during the TAG event. Between these two constraints and the required contact orientation, the spacecraft attitude quickly becomes over-constrained. While gimbals on one or more of these components (camera, array, and antenna) can alleviate the conflicts between these requirements, a carefully designed TAG trajectory may be a viable alternative.

Available Thrust. During the contact phase of a TAG, the spacecraft must reverse its momentum before spacecraft safety is compromised. A maximum allowable contact velocity, v, can be approximated (Eq (1)) as a function of available thrust, T, spacecraft mass, m, and allowable "stroke" or distance to travel, s, while the thrusters reverse the spacecraft's momentum.

$$v^2 = 2\frac{Ts}{m} \tag{1}$$

Contact moments induce an angular rate on the spacecraft that persists after it leaves the surface. Available thrust and thrust duration factor into how large the uncertainty is in the post-ascent spacecraft state.

Fault Protection. Fault protection for TAG, while outside the scope of this paper, is generally different from typical fault protection approaches in that it must be able to respond appropriately should the spacecraft safe while on an impact trajectory. The TAG trajectory design must consider the fault protection mode being used at each phase and take appropriate action. For example, if the response to a safe mode is to execute the ascent burn, the design should not require a spacecraft attitude where an untimely ascent burn execution would endanger the mission.

DESIGN DRIVERS: MISSION OBJECTIVE CONSTRAINTS

A touch-and-go architecture must flow from the mission objectives. These objectives can take the form of science requirements in the case of a science mission, or engineering requirements in the context of a technology-demonstration mission.

Landing Site Location and Contact State Accuracy. The landing site location clearly has a significant impact on all aspects of a TAG trajectory. However, since the surface topography is generally unknown during the planning stages of a mission, the landing site is usually determined during the encounter. The TAG trajectory planning must allow for the range of potential landing sites identified in advance by the mission.

In addition to the spacecraft safety requirements on the size of the landing ellipse and hardware constraints on the contact velocity, the mission objectives may further constrain the allowable variation in the landing ellipse size, dispersions in the velocity at contact, or the time of contact. Examples of motivations include acquiring a sample from a specific location on the surface, the end-effector operates best in a small velocity range, etc.

Contamination. Some sample return science requires pristine or even cryogenic samples be returned to Earth. For missions of this type, the trajectory must be biased in such a way as to not require a burn in the direction of the surface while below some altitude, lest the propellant products or the heat of the plume alter the collected sample. In addition to placing a requirement on the descent trajectory, such a requirement could also place restrictions on the entire TAG campaign, such as the ability to go to multiple sites on the surface for multiple attempts or rehearsals. Alternately, a contamination requirement could constrain the ascent burn size due to propulsion system choices (e.g. cold gas).

DESIGN CHOICES

The primary products of the trajectory design process are a fuel budget, trajectory geometry, and a timeline of events. These are necessarily statistical estimates due to the uncertainties in the small body target parameters (diameter, mass, rotation rate/pole, etc). In addition, because the landing site is almost certainly unknown *a priori*, the final trajectory to be flown is also unknown *a priori*. The objective of the trajectory design team for a TAG mission is to ensure that when the spacecraft arrives at the small body, it can meet the mission requirements within the available consumables and within the planned timeline regardless of what the target parameters actually are.

Staging. The staging phase is the steady-state portion of the TAG design from which the spacecraft begins its descent to the surface. The staging trajectory geometry and the staging location are two important choices for this phase of the design.

The staging trajectory geometry should ensure that the spacecraft remains on a safe trajectory until descent is willfully initiated. Because of the generally small gravitational pull of these bodies and the perturbed dynamical environment, a number of station-keeping options may be appropriate for staging. Options include a stable orbit, an unstable orbit with station-keeping maneuvers, orbit segments connected by maneuvers (a.k.a. "ping-ponging"), "hovering" at a fixed position with a dead-band thrust control,[31] and everything in-between. Choice of a geometry will depend on the dynamical environment (some options may be precluded), the spacecraft and ground system capabilities, compatibility with the descent strategy, and ability to verify hardware operation (if necessary).

The choice of staging location (i.e., range and solar phase angle) must ensure that sufficient time exists to perform all spacecraft and ground functions needed in advance of descent in a timely manner considering ground decision/design turnover times, light times, and the dynamics. The staging location choice, being the gateway between TAG and the rest of the mission, may also be influenced by other mission objectives, such as remote sensing before and after TAG, or by the need for TAG sensor checkouts before descent. As such, sensor ranges may be a consideration in the altitudes and solar phase angles at which the staging phase takes place.

Descent. In the descent phase, the spacecraft begins and ends its motion toward the surface and includes all of the maneuvers after staging that are required to reach the targeted contact state and time. Design of these maneuvers is driven by the dynamics, the targeted contact state, and the geometrical constraints placed upon the spacecraft attitude. In addition, they must meet the requirements placed upon them, such as contamination avoidance. Adding more maneuvers adds execution errors to the dispersions in the contact state, but they also provide opportunities to clean up accumulated maneuver execution, navigation, and dynamical errors. The choice of navigation architecture (e.g., autonomous vs. ground-in-the-loop) drives the number of maneuvers that can be done and the timeliness of navigation data, which directly affects the contact state dispersion. The time to descend also must be chosen and may be driven by the contact velocity to be achieved, the rotation rate of the body or secondaries, or the battery lifetime of the spacecraft.

One major feature of the descent phase is whether or not it contains a "passive abort" such that the spacecraft would not contact the surface without a subsequent command from the ground. This maneuver is sometimes referred to as a "drop burn," or a "commit burn." The primary reason a passive abort is desired is for spacecraft safety and a desire for an operational rehearsal of some portion of the TAG trajectory. A passive abort may not be desired if it is too expensive in terms of fuel, if the Earth-spacecraft distance is too large for ground-in-the-loop commanding, or if the risk of the operational complexity of ground-in-the-loop is judged to be greater than the risk of an off-nominal contact with the surface.

Contact. The contact phase is the shortest phase of the TAG trajectory design. It lasts only a few seconds, but the 6-DOF dynamics introduced by interaction with the surface are complex. The contact phase duration is driven by the contact velocity (stroke length), the purpose of TAG (sampling, surface property measurement, etc), the device used to achieve that goal, and the thrusters' size. Further, the attitude control system's capabilities, coupled with the torques imparted into the spacecraft from the contact velocity, will determine how much the spacecraft attitude changes during the contact phase and thus drive the ascent design. Cangahuala *et al*[27] gives a more thorough description of the trades and considerations for the contact phase design.

Ascent. Finally, the TAG sequence ends with the ascent phase. The ascent phase begins with an "ascent burn," which is triggered at contact or very shortly thereafter. The two varieties of ascent phase are to either return to the staging phase, or to escape from the small body environment (to return at a later date if required). The ascent burn must be sized to ensure that a re-contact

with the small body does not occur until an acceptably long time has passed, including the effects of attitude and rate disturbances during contact. In general, this duration should be long enough for ground commanding and safe mode recovery.

In addition to the whether or not the spacecraft directly returns to staging or not, the ascent burn can be a single large burn or a series of smaller burns. For example, if the landing site is sensitive to combustion products, the ascent burn could use a cold-gas system to get far enough above the landing site before activating a hydrazine system to complete the ascent.

HISTORICAL PRECEDENTS AND CASE STUDIES

The preceding discussion has been, of necessity, very generalized. The array of constraints, requirements, and dynamic environments can vary as much as the possible target bodies themselves do. In this section, we describe, through the lens of the above discussion, the two historical missions (NEAR-Shoemaker and Hayabusa) that designed and implemented asteroid landings. The Hayabusa mission at Itokawa was a true TAG trajectory design, though it remained on the surface longer than intended. The NEAR-Shoemaker extended mission to land on Eros was just that, a landing. No ascent was attempted.

In addition to the two historical missions, where we are limited in our ability to know what the trajectory designers were thinking, three case studies of TAG trajectory design are discussed: the Martian moon Deimos; an active Jupiter family comet, Tempel 1; and a binary near-earth asteroid, 1996 FG3. These are summarized in Table 1.

Table 1: Historical Precedents and Case Study Summaries

Mission/Target	Target Body Summary	Staging	Descent	Ascent
NEAR-Shoemaker Landing on Eros	Large small body (33 km in largest dimension) weak SRP	Retrograde equatorial orbit	No passive abort with horizontal velocity biasing	N/A
Hayabusa TAG on Itokawa	Very small body (0.5 km in largest dimension), strong SRP	Earth-line vertical hovering	No passive abort with autonomous cross-track control.	To staging
Deimos	Medium size body (15 km diameter), dominated by Mars tides	Distant retrograde orbit	Passive abort with horizontal velocity cancellation and limited autonomy	Escape
Comet Tempel 1	Active Jupiter-family comet with known shape (6.0 km mean diameter)	Hyperbolic flyby	Passive abort; fully autonomous descent with sensitivity to contamination	Escape
1996 FG3	Small body (1.8 km diameter), fast rotator, small moon	Horizontal sunline hover	Passive abort with periodic Coriolis cancellation during fully autonomous descent and sensitivity to contamination.	To staging

Historical Precedent: NEAR-Shoemaker Landing on Eros

The February 2001 NEAR-Shoemaker landing on Eros was not a touch-and-go trajectory, but the trades the design team undertook are instructive. The main differences, from a design standpoint, between the TAG architecture and the NEAR-Shoemaker experience is that the NEAR-Shoemaker spacecraft was not designed to make contact with the surface of Eros and spacecraft safety and survivability was a secondary concern to the design team. The primary purpose of the landing attempt was to generate as much imagery at close range as possible. For a full description

of the NEAR-Shoemaker landing on Eros, we recommend Antresian, *et al*[32], Veverka, *et al*[33], and Antresian, *et al*[34].

The NEAR-Shoemaker landing on Eros began with a stable, near circular, equatorial and retrograde 35 km radius orbit. Eros itself is approximately 34 x 11 x 11 km in extent. A hover was considered and rejected due to the large fuel requirements; the spacecraft, which had already been launched and was operating when the decision to land had been made, had limited fuel available with which to attempt a landing. The descent phase included five "end-of-mission maneuvers," or EMMs, which targeted a landing site in the saddle of Eros. EMM-1 altered the inclination of the orbit and put the spacecraft on an impact trajectory. EMM-2 zeroed the horizontal velocity at 12.2 km radius, while it and EMMs 3 and 4 lofted the trajectory slightly while keeping the spacecraft on an eventual impact trajectory. These lofting (or "bouncing") maneuvers were included in the design to extend the descent phase duration, and required the ground to upload a timing update based on the execution errors from EMM-1. Absent this update, the lofting aspect of the maneuvers could cause the spacecraft to be on an escape trajectory. This timing update had to occur in the 3.75 hours between the execution of EMM-1 and EMM-2 and had to include slews between the burn attitudes and Earth-pointing, reacquisition of signal by the Deep Space Network (DSN) antennas, radiometric and optical data acquisition and processing, and the generation of the update itself. An autonomous approach was considered and rejected because it would have required significant re-writing of spacecraft flight software. EMM-5 was designed to minimize the landing velocity (approx. 2 m/s) and bias the horizontal velocity to increase the chances that the spacecraft would land upright, which it ultimately did.

The design of the descent trajectory was highly constrained by the need to keep the high-gain antenna within 1 deg of Earth and the multi-spectral imager nearly normal to the surface, except during burns. Both the antenna and the imager were body-mounted to the spacecraft, so this severely limited the accessible landing sites.

Historical Precedent: Hayabusa TAG at Itokawa

The Japanese mission Hayabusa performed a touch-and-go at the asteroid Itokawa on November 19th and 25th, 2005. The navigation, guidance, and control of the TAG phase has been the subject of many papers, particularly Kawaguchi[35], Kawaguchi *et al*[36], Morita *et al*[37], and Hashimoto *et al*[38]. Though the mission did not achieve all that it set out to do as far as a touch-and-go was concerned (it aborted on November 19th before reaching the surface and remained on the surface for over 30 minutes on the second attempt), the design choices the JAXA team made are instructive nonetheless.

Itokawa is approximately 535 x 294 x 209 meters in extent and was approximately 1 AU from the sun in November 2005 with a one-way light time of approximately 16 minutes. At that size and distance from the sun, orbiting the asteroid is infeasible; the SRP/gravity ratio is simply too large. Therefore, a hovering staging phase was the only choice for the Hayabusa designers. Hayabusa operated by hovering above Itokawa along the Earth line such that almost all of the stationkeeping motion could be detected and controlled using Doppler-effect radiometric data only. The descent phase was simply an extension of this stationkeeping box toward the surface of Itokawa, with plane-of-sky control coming from autonomous on-board tracking of an artificial landmark previously deployed during the mission. Ground controllers observed real-time residuals of the Doppler tracking data and manually adjusted the descent rate to ensure that Hayabusa contacted the desired location on Itokawa with acceptable velocity when the site rotated beneath the Earth line on its 12-hour "day." This approach was constrained to landing sites that rotated through the Earth-line. When ground-controllers elected to continue after an anomaly on November 25th, the autonomous ascent burn was inadvertently disabled. Not until after ground controllers saw the

descent rate change in the real-time residuals was the ascent command sent. The planned ascent was the reverse of the descent; the spacecraft ascended from the surface along the Earth line and the stationkeeping box was re-established.

Case Study: Deimos

Deimos, the further out and smaller of the moons of Mars, is 15 x 12.2 x 10.4 km in extent, has a gravitational constant of 9.85e-5 km^3/s^2, and has been extensively imaged by the Viking orbiters and other spacecraft. It is in a 30.3 hour orbit about Mars and is tidally locked. The assumed TAG design requirement was for a 0.05 to 0.30 m/s contact at any reachable point on Deimos with minimal horizontal contribution. Further, because full autonomy was prohibitively expensive for this concept, ground-based optical navigation was required for the main descent phase. An autonomous correction to the drop burn was acceptable, but certain biases were required to keep the correction within the capability of the limited autonomous system.

The Deimos TAG trajectory design concept is shown schematically in Figure 4. The staging phase is a 20 x 24 km equatorial distant retrograde orbit (DRO). The descent phase includes a small maneuver to place the spacecraft on a 500 meter, 5 m/s flyby above the surface 4.5 hours after the descent burn. During the intervening time, ground-based radiometric and optical navigation updates the remaining burns in the descent using a NEAR-like approach. The next burn in the descent is a two-part zeroing of the horizontal velocity at 500 meters (the "drop burn"). The second part, 10% of the total, cleans up the first part of the burn. The 0.17 m/s contact velocity is controlled by a pair of braking maneuvers triggered by a radar altimeter. At the moment of contact, a large ascent burn places the spacecraft in a Deimos-leading orbit.

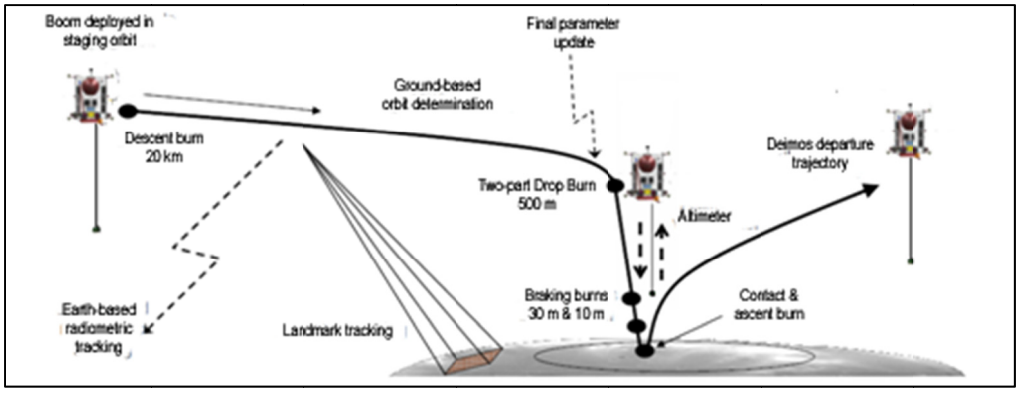

Figure 4. Deimos TAG Trajectory Design Concept

Staging Design. The DRO was selected because Mars tides dominate most motion around Deimos, and other orbits were either unstable due to these tides or were too close to Deimos and thus unstable due to its non-sphericity. The orbit was high enough that the descent phase took long enough for the ground-based navigation to take place (4.5 hours, with a one-way light time of 18 minutes), but not so high that execution errors in the drop burn would exceed the capability of the autonomous correction burn.

Descent Design. The passive-abort option was selected due to a requirement that the altimeter lock onto the surface before the spacecraft was placed on an impact trajectory. The two-part drop burn was selected because the execution errors in a single, large burn were excessive and had to be corrected if the horizontal velocity requirement was to be achieved. In order to perform the cleanup (which had to be autonomous due to the round-trip light-time), the spacecraft would have had to yaw to place the thrusters in the correct direction. The 90/10 split resulted in sufficiently

small yaws after a Monte Carlo analysis was performed. The two braking burns, which brought the spacecraft to nearly to rest at 30 and 10 meters altitude, were selected to control both the contact velocity and the dispersions on it without introducing additional, uncorrectable horizontal velocity errors.

Contact Design. The assumed requirement for an over-flight of the TAG site during rehearsals of the descent, coupled with the tides-dominated dynamics, constrained the landing site to be near either the sub-Mars or anti-Mars points on Deimos. Locations on the leading or trailing edge could have been reached, but the fuel requirements to fly over the poles of Deimos were larger than desired, as those trajectories required plane changes in Mars orbit and the DRO began to lose stability with larger inclinations.

Ascent Design. The ascent burn was sized to escape because the large attitude excursions (5 deg, 4 deg/sec) expected due to the high torques imparted by the contact event could be in any direction and anything smaller could re-contact the surface at unpredictable times. By sizing the burn to escape and using the burn controller to null the rates, the large uncertainty in the burn direction was nullified. Returning to the staging orbit was then a simple matter of reversing the drift-away rate and re-inserting into the DRO.

Case Study: Comet Tempel 1

Tempel 1 is a Jupiter family comet that was visited by the Deep Impact mission.[39] A comet sample return concept study has been done at JPL that considered TAG at Tempel 1 during a period of active comet outgassing at 3.0 AU.

The shape of Tempel 1 has been derived from Deep Impact imagery[40] and is approximately 7.4 x 6.2 x 5.4 km in diameter along the principal axes. No mass estimate exists however, so there is significant uncertainty in Tempel 1's gravitational attraction. The outgassing activity of Tempel 1 is expected to be highly variable with respect to time and surface location. When the spacecraft is inside an outgassing "jet", accelerations are expected to be many times the local gravitational acceleration. Given ranges to Earth of ~3.0 ± 1 AU, round-trip communication times are delayed by up to 1 hr.

The TAG trajectory concept developed is illustrated in Figure 5. During the staging portion of the trajectory, the spacecraft approaches Tempel 1 from 120-km range at 3 m/s on a hyperbolic flyby trajectory. One maneuver is executed during approach to correct for statistical errors and an initial close-approach altitude bias. The descent phase begins at 500-m altitude (near close approach), when a maneuver places the spacecraft onto an impact trajectory with the comet surface. During descent, guidance, navigation, and control are performed by an autonomous system ("AutoGNC") using landmark tracking navigation.[28] Opportunities for statistical correction burns occur every 5 minutes on descent. Two braking burns govern descent speed to achieve a targeted vertical touchdown speed of 20 cm/sec.The ascent burn places the spacecraft onto an escape trajectory, where ground operations can take over to resume the mission.

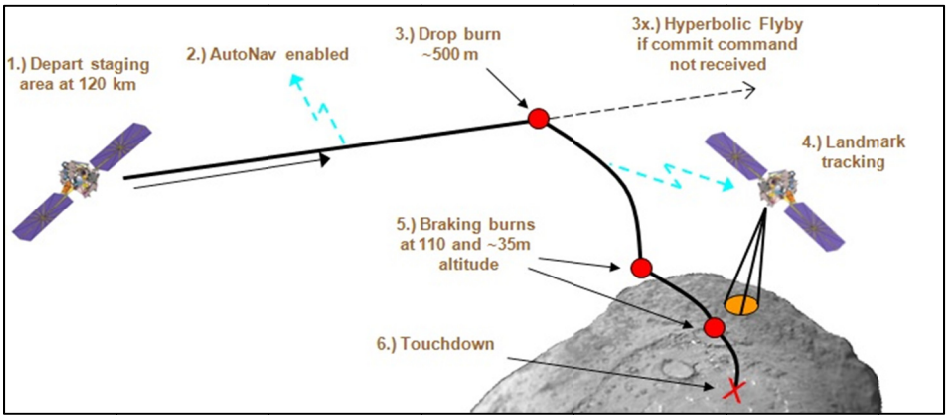

Figure 5. Tempel 1 TAG Trajectory Design Concept

Staging Design. A hyperbolic flyby was planned primarily for its passive abort properties. The ~24 hour time from the start of staging to the drop burn allowed for ground operations to independently verify the first AutoGNC maneuver design (approach bias maneuver) and verify altimeter operations before giving control to AutoGNC shortly before descent began. The speed of approach was dictated by the hyperbolic flyby speed needed for the upper limit of mass possibilities considered for Tempel 1. The small number of maneuvers (i.e., simplicity relative to active station-keeping) and stability properties of the flyby (relative to unstable inclined orbits) were also considered in this choice of staging approach.

Descent Design. Just before descent, the spacecraft was to fold up its solar arrays to prepare for surface interaction. A requirement was levied that the descent/ascent must take place in less than ~45 minutes due to battery power constraints. The drove, in part, the choice of drop burn altitude and residual downward speeds between drop and the first braking burn, and the first and second braking burns. The placement of the first braking burn was selected primarily to minimize surface contamination from the hydrazine burn. The placement of the second braking burn was driven by the desired touchdown speed and ground dispersion sensitivity to errors in this burn. The drop burn altitude was also driven by a desire to confirm proper altimeter operation (max range of ~2 km) with ground in the loop before committing to descent.

Contact Design. The contact location on the surface was to be selected after a remote sensing mission phase. Whatever the location, it was desirable to land in the local morning (to avoid the more intense outgassing expected in the afternoon) at a time with good lighting for imaging.

Ascent Design. A single burn-to-escape from the surface using hydrazine thrusters was selected for ascent for simplicity of operations and spacecraft design. This choice removes the time pressure for resuming operations associated with a non-escape trajectory. The hydrazine ascent outweighed concerns about contamination of the landing site for future TAG attempts because the cost of the needed cold gas thrust system was prohibitive.

Case Study: Binary Asteroid 1996 FG3

Compared to Deimos and Tempel 1 case studies, relatively little is known about 1996 FG3. It is a Class C asteroid,[41] with an absolute magnitude of 18.066 ± 0.59248, a retrograde rotation period of 3.5942 hours, and a small moon. The estimate of the rotation rate comes from two papers published in the same issue of *Icarus* that made different assumptions in processing light curve data. The challenge is then to reconcile the assumptions and come to a single set of system constants.

Mottola and Lahulla[42] assumed that the Secondary is in a circular orbit about the Primary and calculated the system orbit pole, the system orbit period, the system orbital radius, the spin rate of the Primary and the shapes of both bodies. They further assumed that the minor and intermediate axes of the Secondary were of the same value. They reported all the lengths as normalized distances, but never defined what the normalizing distance was. Pravec *et al*[43]. assumed that both bodies were spheres and calculated the system orbit period, the system orbital radius, the spin rate of the Primary, the system eccentricity, and the radius of the Primary. They further assumed a geometric albedo of 0.06 and thus reported all the distances in km. Both papers calculated the orbit period to be 16.135 hours. To reconcile the different shape models arrived at by the two papers, a reasonable value for the undefined Mottola and Lahulla normalizing distance was determined to be 0.720 km. This value is then used to convert the Mottola and Lahulla distances into physical parameters, as reported Table 2. Unfortunately, because of the assumption of the geometric albedo, there is a factor of $\sqrt{2}$ uncertainty in the normalizing distance. The effect of this uncertainty on the system constants are also reported in Table 2.

Table 2: Derived 1996 FG3 System Constants

	Nominal	Maximum	Minimum	
Normalizing Distance	0.720	1.02	0.509	km
Primary Ellipsoid				
Major Axis	0.756	1.07	0.535	km
Intermediate Axis	0.684	0.968	0.484	km
Minor Axis	0.504	0.713	0.357	km
Secondary Ellipsoid				
Major Axis	0.231	0.326	0.163	km
Intermediate Axis	0.166	0.234	0.117	km
Minor Axis	0.166	0.234	0.117	km
Secondary Orbit				
Semi-Major Axis	2.09	2.95	1.48	km
Period	58086	58086	58086	sec
System Parameters				
Primary GM	1.04E-07	2.95E-07	0.368E-07	km^3/sec^2
Secondary GM	2.52E-09	7.14E-09	0.892E-10	km^3/sec^2

Given the unknown topography, an attempt was made to estimate the likelihood that there would be available landing sites on the surface of this small of a body. To perform this analysis requires a boulder density. One possible distribution is the one documented for the asteroid Itokawa,[44,45] as in Eq (2):

$$N = 48000D^{-2.8} \tag{2}$$

where D is the boulder diameter and N is the number of boulders whose size is greater than or equal to D.

Using this boulder distribution and an asteroid area, simulated boulder fields were created. To compare the sensitivity to the assumed boulder distribution, the distribution was scaled to produce different cumulative fractional areas (CFAs) covered by 1-meter and larger boulders. The simulated boulder fields were then searched for non-overlapping circular footprints 95% free of 1-meter boulders. The results of the footprint search are shown in Table 3, which suggests that for circular footprints of 5.0 meters radius or larger, it is very unlikely a suitable landing site exists. However, the analysis did not take into account the natural sorting mechanisms on asteroids that can produce relatively smooth areas. For example, Figure 6 shows a 5-meter radius region on a

high resolution Itokawa image that is clearly free of large boulders. Regardless, the analysis indicated that having as small a landing ellipse as possible was desirable. This is especially true when considering that an ideal landing site can be overly constrained by both engineering considerations (i.e. safety requirements) and science considerations (i.e. sites that meet science requirements).

Table 3: Number of non-overlapping footprints found as a function of rock field CFA and circular footprint radius

# of non-overlapping TAG sites for a given footprint size and CFA*		Footprint Radius (meters)		
		3.3	5.0	50.0
Rock Field CFA of 1-meter and larger	10%	33,085	27,039	264
	15%	15,275	14,082	0
	20%	5,142	4,164	0
	25%	862	361	0
	30%	107	9	0
	33% (Itokawa)	19	0	0

*Selected sites are 95% free of rocks larger than 1-m

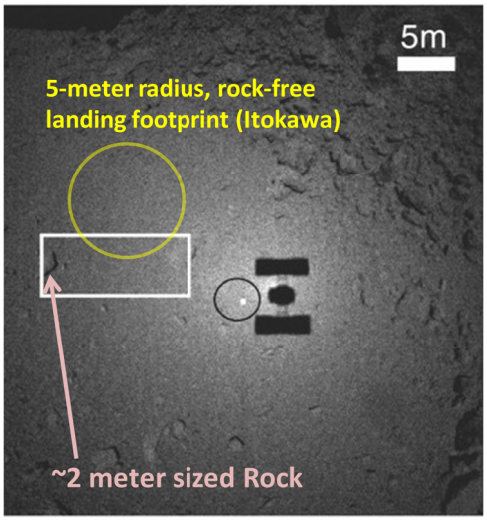

Figure 6: Sample 5-meter radius footprint on Itokawa

The TAG design concept for 1996 FG3 is illustrated in Figure 7. The spacecraft begins in a 5 km radius sun-line horizontal ping-pong hover. The descent burn targets 210 meter altitude flyby approximately over the targeted contact site. After the descent is verified on the ground, an autonomous navigation and control system**Error! Bookmark not defined.** is activated to fly the descent and ascent phases. The remainder of the descent phase was designed to keep the landing site within a camera field of view while spacecraft pitched over at a rate equal to the asteroid rotation and to keep the thruster plumes off the surface. A few seconds after contact, the ascent burn is initiated and designed to return the spacecraft above the orbit of the secondary within a few hours. The entire TAG trajectory had to occur within 8 hours to ensure that the Secondary remained on the far side of the Primary during the trajectory.

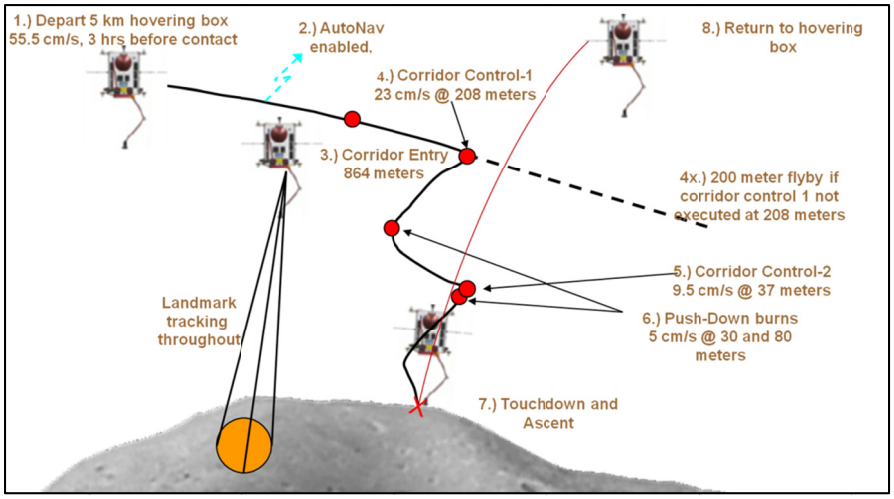

Figure 7. 1996 FG3 TAG Trajectory Design Concept

Staging Design. A 5 km radius, ±45 deg off the sun-line hover was used for the staging phase to simplify the phasing of the local solar time of the landing point (3.6 hours) and the orbit of the secondary (16.1 hours). The 5 km radius was chosen to match the instrumentation, as a 5 km orbit was used in the pre-TAG campaign. However, this orbit had a 150 hour period, and the operational complexity of compensating for all three periods in deciding when to attempt a TAG was judged greater than the complexity of the active hovering scheme.

Descent Design. A pair of corridor-control burns was required to counter the large Coriolis effect in the surface-relative dynamics and maintain the landing site within the camera field of view requirement. In addition to these burns, a pair of 5 cm/s "push-down" burns were included in the design to bias the trajectory such that the clean-ups would not result in burns toward the surface, violating the sample contamination requirement.

Contact Design. Context imaging of the sampling site required that contact occur in either local mid-morning or afternoon. The mid-morning contact time was selected because the mid-afternoon contact time would place the beginning of the descent over the night-side of the target (though not in eclipse), which was undesirable from an optical navigation standpoint.

Ascent Design. The ascent burn is a 0.6 m/s burn sized to ensure that even in the presence of the largest attitude excursions due to contact would result in a return to 5 km altitude within the five hours remaining. Without any excursions, the result is a return to the staging area within three hours. If the autonomous navigation system did not re-insert into the staging hover, the spacecraft would be on an escape trajectory and the hover could be re-established via ground commands at any later date.

CONCLUSIONS

The trajectory design process for a "touch-and-go" (TAG) mission to the surface of small body must consider many factors before arriving at a workable solution. An expansive set of common TAG trajectory design drivers are discussed from the areas of spacecraft dynamics, small-body environment, spacecraft and ground system capabilities, and mission objectives. The discussion of design choices and the case study designs presented provide examples of how the design drivers might apply. This paper provides a trajectory designer or systems engineer with a high-level understanding of the factors that affect and limit TAG trajectory design and a number of references for more-detailed further study.

ACKNOWLEDGEMENTS

The research was carried out at the Jet Propulsion Laboratory, California Institute of Technology, under a contract with NASA.

REFERENCES

[1] National Research Council of the National Academies, Space Studies Board. "New Frontiers in the solar system: An Integrated Exploration Strategy." The National Academies Press, Washington, D.C., 2003

[2] National Aeronautics and Space Administration, "2006 Solar System Exploration Roadmap Report for NASA's Science Mission Directorate," September 2006.,
http://solarsystem.nasa.gov/multimedia/downloads/SSE_RoadMap_2006_Report_FC-A_opt.pdf

[3] Office of the President of the United States, "National Space Policy of the United States of America," 28 June 2010, http://www.whitehouse.gov/sites/default/files/national_space_policy_6-28-10.pdf

[4] National Aeronautics and Space Administration, "Exploration of Near Earth Objects Objectives Workshop Summary Report, 20 September 2010, http://www.nasa.gov/pdf/483296main_20100920-Explore_NOW_Summary_Report.pdf

[5] Scheeres, D.J. "Dynamics About Uniformly Rotating Tri-Axial Ellipsoids: Applications to Asteroids," *Icarus*, Vol 110, 1994, pp. 225-238.

[6] Scheeres, D.J. and Marzari, F., "Spacecraft Dynamics in the Vicinity of a Comet," *Journal of the Astronautical Sciences*, Vol 50, 2002, pp 35-52.

[7] Scheeres, D.J., et al, "Evaluation of the Dynamic Environment of an Asteroid: Applications to 433 Eros," *Journal of Guidance, Control, and Dynamics*, Vol 23, 2000, pp 466-475.

[8] Scheeres, D.J, et al, "Orbit Mechanics About Small Bodies," paper AAS 09-220, AAS/AIAA Spaceflight Mechanics Meeting, February 2009, Savannah GA.

[9] Byram, Sharyl M., et al, "Models for the Comet Dynamical Environment," *Journal of Guidance, Control, and Dynamics*, Vol 30, 2007.

[10] Kaula, William M. Theory of Satellite Geodesy, Applications of Satellites to Geodesy. Dover Publications, Inc. Mineola, New York, 1966

[11] Weeks, Connie, and Miller, James K. "A Gravity Model for Navigation Close to Asteroids and Comets," *The Journal of the Astronautical Sciences*, Vol. 52, 2004, pp. 381-389.

[12] Werner, R.A. "The Gravitational Potential of a Homogenous Polyhedron, or Don't Cut Corners," *Celestial Mechanics & Dynamical Astronomy*, Vol. 59, 1994, pp. 253-278.

[13] Meirovitch L., *Methods of Analytical Dynamics*, McGraw Hill, New York, 1970.

[14] Scheeres, D.J. "Satellite Dynamics About Asteroids," *Advances in the Astronautical Sciences,* Vol 87, 1994, pp. 275-292.

[15] Scheeres, D.J., "Satellite Dynamics about Small Bodies: Averaged Solar Radiation Pressure Effects," *Journal of the Astronautical Sciences*, Vol 47, 1999, pp 25-46

[16] Broschart, S.B., et al, "New Families of Multi-Revolution Terminator Orbits Near Small Bodies" paper AAS 09-402, AAS/AIAA Astrodynamics Specialists Meeting, Pittsburgh, PA, August 2009.

[17] Szebehely, V. Theory of Orbits. The Restricted Problem of Three Bodies, Academic Press, New York, 1967, Sections 1.1-1.10, 8.1, 10.4

[18] Bellerose, Julie, and Scheeres, Daniel J., "Restricted Full Three-Body Problem: Application to Binary System 1999 KW4," *Journal of Guidance, Control, and Dynamics*, Vol 301, 2008, pp 162-171.

[19] Fahnestock, E.G., and Scheeres, D.J., "Simulation and analysis of the dynamics of binary Near-Earth Asteroid (66391) 1999 KW4," *Icarus*, Vol 194, 2008, pp. 410-435.

[20] Fowler, J. W. & Chillemi, J. R.The IRAS Minor Planet Survey (Tech. Rep. PL-TR-92-2049 1992, IRAS Asteroid Data Processing, ed. E. F. Tedesco, G. J. Veeder, J. W. Fowler, & J. R. Chillemi (Hanscom AF Base, MA: Phillips Lab)

[21] Hudson, S., "Three-dimensional Reconstruction of Asteroids from Radar Observations." *Remote Sensing Reviews*, Vol 8, 1993, pp 195-203

[22] Hamilton, Douglas P., and Burns, Jospeh A., "Orbital Stability Zones about Asteroids," *Icarus*, Vol 92, 1991, pp 118-131.

[23] Hamilton, Douglas P., and Burns, Jospeh A., "Orbital Stability Zones about Asteroids, II. The Destabilizing Effects of Eccentric Orbits and of Solar Radiation," *Icarus*, Vol 96, 1992, pp 43-64.

[24] Hu, W. and Scheeres, D.J., "Numerical Determination of Stability Regions for Orbital Motion in Uniformly Rotating Second Degree and Order Gravity Fields," *Planetary and Space Science*, Vol 52, 2004, pp 685-692.

[25] Fahnestock, Eugene G., et al, "Surface Impact or Blast Ejecta Behavior in a Small Binary Asteroid System with Application to In-Situ Observation," *Proceedings of the 2010 AAS/AIAA Space Flight Mechanics Conference*, San Diego, CA, 14-17 February, 2010

[26] Geissler, Paul, et al, "Erosion and Ejecta Reaccretion on 243 Ida and Its Moon" *Icarus*, Vol 210, 1996, pp 140-157.

[27] Cangahuala, L. A., et al, "GN&C Trades for Touch-and-Go Sampling at Small Bodies," AAS Guidance and Control Conference, 4-9 February 2011, Breckenridge, CO

[28] Bhaskaran, Shyam, et al. "Small Body Landings Using Autonomous Onboard Optical Navigation," Born Symposium, Denver, CO, May 13-14, 2010.

[29] Owen, et al, "NEAR Optical Navigatin at Eros," paper AAS 01-376, AAS/AIAA Astrodynamics Specialist Conference, Quebec City, Quebec, Canada, July 30-August 2, 2001.

[30] Owen, W.M., Jr., "Methods of Optical Navigation," paper AAS 11-215, AAS/AIAA Spaceflight Mechanics Conference, New Orleans, LA, 13-17 February 2001.

[31] Broschart, S. B. and Scheeres, D. J., "Boundedness of Spacecraft Hovering Under Dead-Band Control in Time-Invariant Systems" *Journal of Guidance, Control, and Dynamics*, Vol 30, 2007, pp 601-610.

[32] Antresian, P. G., et al, "The Design & Navigation of the NEAR Shoemaker Landing on Eros," paper AAS 01-372, AAS/AIAA Astrodynamics Specialists Conference, Quebec City, Quebec, Canada, July 30-August 2, 2001.

[33] Veverka, J., et al, "The landing of the NEAR-Shoemaker spacecraft on asteroid 433 Eros," *Nature*, Vol 413, 27 Sep 2001, pp 390-393

[34] Antresian, P.G., et al, "NEAR Shoemaker's low altitude operations at EROS," presented at the International Symposium on Space Flight Dynamics, Pasadena, CA, 3 Dec 2001

[35] Kawaguchi, Jun'ichirco, "Hayabusa, Summary of Guidance, Navigation and Control Achievement in its Proximity Phase," paper AIAA 2006-6533, AIAA/AAS Astrodynamics Specialist Conference, Keystone, CO, 21-24 August, 2006.

[36] Kawaguchi, Jun'ichiro, Aida, Saika, and Morita, Hideo, "Hayabusa, Detailed Guidance and Navigation Operations during Descents and Touchdowns," paper AIAA 2006-6536, AIAA/AAS Astrodynamics Specialist Conference, Keystone, CO, 21-24 August, 2006.

[37] Morita, Hideo, et al, "Hayabusa's Real-time Landmark Tracking Navigation for Descents and Touching-Downs," paper AIAA 2006-6537, AIAA/AAS Astrodynamics Specialist Conference, Keystone, CO, 21-24 August, 2006.

[38] Hashimoto, T., et al, "Final Autonomous Descent Base on Target Marker Tracking," paper AIAA 2006-6538, AIAA/AAS Astrodynamics Specialist Conference, Keystone, CO, 21-24 August, 2006.

[39] A'Hearn, M.F. et al., "Deep Impact: Excavating Comet Tempel 1," *Science*, Vol 310, 2005, pp 258-264,

[40] Thomas, Peter C., et al., "The shape, topography, and geology of Tempel 1 from Deep Impact observations" *Icarus,* Vol. 191, 2007, pp. 51-62.

[41] Neese, C., Ed., Asteroid Taxonomy V6.0. EAR-A-5-DDR-TAXONOMY-V6.0. NASA Planetary Data System, 2010

[42] Mottola, Stephano, and Lahulla, Felix, "Mutual Eclipse Events in Asteroidal Binary System 1996 FG3: Observations and Numerical Model", *Icarus*, Vol. 146, 2000, pp. 556-567.

[43] Pravec, Petr, et al., "Two-Period Lightcurves of 1996 FG3, 1998 PG, and (5407) 1992 AX: One Probable and Two Possible Binary Asteroids", *Icarus*, Vol. 146, 2000, pp. 190-203.

[44] Saito, J., et al "Detailed Images of asteroid 25143 Itokawa from Hyabusa," *Science*, Vol 312, 2006, pp. 1341-1344

[45] Miyamoto, H., et al, "Regolith migration and sorting on asteroid Itokawa" *Science*. Vol 316, 2007, pp. 1011-1014.